Kappa and other nonequilibrium distributions from the Fokker-Planck equation and the relationship to Tsallis entropy

Bernie D. Shizgal
Department of Chemistry, University of British Columbia, Vancouver, British Columbia, Canada V6T 1Z1

(Received 6 April 2018; published 31 May 2018)

This paper considers two nonequilibrium model systems described by linear Fokker-Planck equations for the time-dependent velocity distribution functions that yield steady state Kappa distributions for specific system parameters. The first system describes the time evolution of a charged test particle in a constant temperature heat bath of a second charged particle. The time dependence of the distribution function of the test particle is given by a Fokker-Planck equation with drift and diffusion coefficients for Coulomb collisions as well as a diffusion coefficient for wave-particle interactions. A second system involves the Fokker-Planck equation for electrons dilutely dispersed in a constant temperature heat bath of atoms or ions and subject to an external time-independent uniform electric field. The momentum transfer cross section for collisions between the two components is assumed to be a power law in reduced speed. The time-dependent Fokker-Planck equations for both model systems are solved with a numerical finite difference method and the approach to equilibrium is rationalized with the Kullback-Leibler relative entropy. For particular choices of the system parameters for both models, the steady distribution is found to be a Kappa distribution. Kappa distributions were introduced as an empirical fitting function that well describe the nonequilibrium features of the distribution functions of electrons and ions in space science as measured by satellite instruments. The calculation of the Kappa distribution from the Fokker-Planck equations provides a direct physically based dynamical approach in contrast to the nonextensive entropy formalism by Tsallis [J. Stat. Phys. **53**, 479 (1988)].

DOI: 10.1103/PhysRevE.97.052144

I. INTRODUCTION

Nonequilibrium effects occur for many physical systems and are often characterized by the departure of the particle translational distribution functions from Maxwellian. A few examples of such systems include irreversible transport processes [1,2], plasma physics [3], reactive systems [4,5], nucleation [6,7], atmospheric and space physics [8,9], shock phenomena [10], neutron transport [11], electron and ion transport [12,13], semiconductor physics [14,15], astrophysics [16,17], as well as finance and social dynamics [18,19]. In every application, the systems of interest can be multidimensional and may depend on several physical parameters. In general, these systems are studied with a variety of transport equations that include the Boltzmann equation, the Fokker-Planck equation, the Vlasov equation, or a master equation. The references cited provide just a few examples of the many theoretical approaches to describe nonequilibrium processes. The Tsallis approach [20–22], based on the definition of an entropy functional characterized by a single parameter q cannot describe the multitude of phenomenon referred to in this paragraph and many others too numerous to list.

The nonextensive approach by Tsallis is based on the definition of an entropy functional of the form

$$S(q) = \frac{1}{q-1}\left[1 - \int f^q(v)d\mathbf{v}\right], \tag{1}$$

parametrized with q. In the limit $q \to 1$, we have with l'Hopital's rule that $\lim_{q\to 1} S(q) \to -\int f\ln(f)d\mathbf{v}$ which is the basis for Boltzmann's H theorem for a dilute monatomic gas [23] and the approach to Maxwellian at equilibrium. For systems with discrete quantum energy levels, the integral is replaced by a summation and the equilibrium distribution is generally referred to as the Maxwell-Boltzmann distribution. The equilibrium distributions are obtained by finding the extremum of the entropy subject to the known values of the density and average energy with the method of Lagrange multipliers. The Tsallis formalism has been widely adopted in space physics as a rationale for the many satellite verifications of particle energy distributions as the Kappa distribution [24–29] given by

$$f_\kappa(x) = C(\kappa)\left[\frac{1}{1+\frac{x^2}{\kappa+1}}\right]^{\kappa+1}, \tag{2}$$

where $x = v/v_{th}$ is the reduced particle speed and $v_{th} = \sqrt{2kT_b/m}$ is the thermal speed with k being the Boltzmann constant and m being the particle mass. The heat bath temperature is denoted T_b. The Kappa distribution is normalized according to $4\pi\int_0^\infty f_k(x)x^2dx = 1$ so that $C(\kappa) = \Gamma(\kappa+1)/\{\Gamma(\kappa-\frac{1}{2})[\sqrt{\pi(\kappa+1)}]^3\}$. It has an asymptotic power law dependence for large speed x and joins smoothly with a Maxwellian distribution at low speed. The Kappa distribution is the single nonequilibrium distribution function obtained by maximizing $S(q)$ as done in equilibrium statistical mechanics [29,30]. The main objective of this paper is to report on the solutions of two different Fokker-Planck equations for the nonequilibrium distribution function of electrons or ions that reduce to the Kappa distribution as solution only for specific system parameters. There are two parameters in the

Fokker-Planck equations used, as explained in Secs. II A and III A.

There is an extensive literature, too large to discuss here (see the bibliography in Refs. [24–29]), in which the authors suggest that the justification for the Kappa distribution (especially in space physics) is the maximization of $S(q)$, Eq. (1), as in the Boltzmann H Theorem. The physical reasons given are many and include long-range forces [31], nonextensive thermostatics [32,33], intermittency [25], a collisionless weakly coupled plasma far from equilibrium [27,28], multiplicative noise [34], Levy flights [35], turbulent fluctuations [36], and other mechanisms. A detailed account of these discussions is provided elsewhere [26–29]. The dependence on κ in Eq. (2) arises from the steady-state solution of a Fokker-Planck equation in terms of a single parameter [see Eq. (7)]. This differs from other forms [25,37] and changes the relationship between the temperature and κ as well as the norm. A more direct approach is the works that demonstrate that the underlying source of the Kappa distribution are wave-particle interactions [38–42] described by an appropriate Fokker-Planck equation. The work by Ma and Summers [38] on Whistler-mode waves [Eqs. (3)–(10)], Hasegawa *et al.* [39] on a radiation field [Eq. (17)], Biró and Jakovác [34] with a Fokker-Planck equation with multiplicative noise [Eqs. (8), (14), and (17)], Lutz [43] [Eqs. (1)–(3)], and Yoon [44] [Eqs. (3)–(10)] for electrostatic Langmuir turbulence, have all demonstrated Kappa distributions as the steady-state distributions of a Fokker-Planck equation [42]. A close examination of all these works shows that they are equivalent in the sense that the Kappa distribution arises from the same velocity variation of the ratio of drift and diffusion coefficients in the Fokker-Planck equations that were used. The current paper demonstrates that it is the particular velocity dependence of the drift and diffusion coefficients in the Fokker-Planck equation that uniquely defines the Kappa distribution irrespective of the actual wave-particle mechanism invoked. The main objectives of this paper is to describe the time evolution of two different systems from an initial Maxwellian distribution to a nonequilibrium steady-state distribution. Two different physical problems each modelled with a two-parameter Fokker-Planck equation are studied.

The first model system, discussed in Sec. II, involves a charged test particle of mass m dilutely dispersed in a second charged species of mass M that acts as a constant temperature heat bath. The two species interact via Coulomb collisions and the test particles are perturbed from equilibrium owing to wave-particle interactions modelled with a diffusion operator. The strength of the wave-particle interaction relative to the strength of Coulomb collisions is given by α. The test particle distribution function is given by a Fokker-Planck equation with both Coulomb collisions and wave-particle diffusion [45,46]. The time evolution of the distribution function to a steady nonequilibrium distribution function is considered for an initial Maxwellian.

The Kullback-Leibler entropy

$$\Sigma_{\rm KL}(t) = -4\pi \int_0^\infty f(v,t) \ln\left[\frac{f(v,t)}{f_{ss}(v)}\right] v^2 dv \qquad (3)$$

is used to rationalize the approach to a steady nonequilibrium distribution function, where $f_{ss}(v)$ is the steady-state distribution. One can show that $d\Sigma_{\rm KL}(t)/dt > 0$ and that $\Sigma_{\rm KL}(t) \to 0$ as $t \to \infty$ [46]. The Kappa distribution arises only for particular system parameters, m/M and α. Otherwise, the nonequilibrium steady-state distributions are not Kappa distributions. The Kullback-Leibler entropy measures the departure of one distribution, $f(v,t)$, from a reference distribution, $f_{ss}(v)$. The difference of the two distributions is often referred to as the Kullback-Leibler distance (see Ref. [47] and references therein).

The second model system discussed in Sec. III concerns the distribution function of electrons dilutely dispersed in a heat bath of a second species. The nonequilibrium distribution function of the electrons is described with a Fokker-Planck equation. We choose a power law momentum transfer cross section, $\sigma(x) = \sigma_0/x^p$, and an electric field parameter β, which is defined later. The velocity distribution function for this physical system is dependent on the physical parameters p and β and has been studied previously [48,49]. The hard sphere cross section corresponds to $p = 0$ and with $p = 1$ we have the Maxwell molecule cross section for scattering from a potential, $V(r) \propto 1/r^4$, familiar from kinetic theory. The Kappa distribution occurs as the steady-state distribution for this system with $p = 2$ and for a limited range of values of the electric field parameter β. It is the Kulback-Leibler entropy that rationalizes the approach to a steady nonequilibrium state and the Tsallis formalism does not play a role.

Numerous researchers [25,27,29,31,32,34] have suggested that the origin of the Kappa distribution can be rationalized with the nonextensive entropy formalism promoted by Tsallis [22,50]. A complete bibliography can be found elsewhere [27–30]. The nonextensive entropy approach to describe this multitude of physical nonequilibrium phenomenon remains controversial as noted by numerous authors [51–60] and others. In the kinetic theory applications discussed here, there is no need to introduce the concept of nonextensive thermodynamics and q-extensive distributions [20]. The steady nonequilibrium distributions for these systems depend on two parameters that characterize the system and a large number of different nonequilibrium steady states are calculated for which the Kappa distribution is found only for a particular choice of these variables.

In Sec. III A, we briefly review the basis for the study of electron thermalization in atomic gases [48,49] and discuss in particular the form of the drift and diffusion coefficients in the Fokker-Planck equation in comparison with recent discussions in the literature for the basis of the Kappa distribution. In Sec. III B, we introduce a model system with a momentum transfer cross section, $\sigma(v) = \sigma_0/v^p$ and based on the Fokker-Planck theory for electron thermalization that describes the relaxation of electrons in a heat bath of atoms and subject to an external electric field of dimensionless strength β [see after Eq. (12)]. We demonstrate that this model can describe electron thermalization to a multitude of different steady-state nonequilibrium distributions and the formation of a Kappa distribution only for specific values of p and β. In each case, we show that the approach to the nonequilibrium steady state is explained with the Kullback-Leibler relative entropy (3). A summary of the results is presented in Sec. IV.

II. SUPRATHERMAL POPULATIONS FOR SPACE PLASMAS AND KAPPA DISTRIBUTIONS

A. Fokker-Planck equation

The Fokker-Planck equation for the relaxation of a charged test-particle of mass m interacting via Coulomb collisions with background charged particles of mass M at equilibrium is given by

$$\frac{\partial f(v,t')}{\partial t'} = \frac{A}{v^2}\frac{\partial}{\partial v}\left[D_1(v)\left(1+\frac{kT_b}{mv}\frac{\partial}{\partial v}\right)\right]f(v,t'), \quad (4)$$

where $A = (4\pi N e^4 Z^2 Z_b^2/mM)\ln\Lambda$ with the diffusion coefficient

$$D_1(v) = \mathrm{erf}\left(\sqrt{\frac{Mv^2}{2kT_b}}\right) - \sqrt{\frac{2Mv^2}{\pi kT_b}}\exp\left(-\frac{Mv^2}{2kT_b}\right), \quad (5)$$

as discussed elsewhere [46,61,62]. Equation (5) arises from the Coulomb cross section for charged particle collisions and is averaged over the Maxwellian distribution function of the background ions. The parameters in A are the density N of the background species, the electronic charge e, the atomic weights Z_b of the background species, and the test particle Z. The Coulomb logarithm is $\ln\Lambda$.

The system described by the Fokker-Planck equation (4) is perturbed with the introduction of an energization mechanism. In the space plasma environment, the energization mechanism could include quasilinear wave-particle interactions modeled by a diffusion in velocity space [38,63–65], so an appropriate FPE is given by

$$\frac{\partial f(v,t')}{\partial t'} = \frac{A}{v^2}\frac{\partial}{\partial v}\left[D_1(v)\left(1+\frac{kT_b}{mv}\frac{\partial}{\partial v}\right)\right]f(v,t') + \frac{B}{v^2}\frac{\partial}{\partial v}\left[v^2 D_2(v)\frac{\partial}{\partial v}f(v,t')\right], \quad (6)$$

where B gives the strength of the wave-particle interaction as modeled with the diffusion coefficient $D_2(v)$.

With the introduction of the dimensionless time, $t = t'/t_0$, where $t_0 = [N\sigma_{\mathrm{eff}}\sqrt{2kT_b/M}]^{-1}$ with $\sigma_{\mathrm{eff}} = [4\pi N Z^2 Z_b^2 e^4 \ln\Lambda]/(2kT_b)^2$ the Fokker-Planck equation (6) can be written in terms of $\alpha = 2B/A$ as a measure of the strength of the wave-particle interaction that energizes the particles. The Fokker-Planck equation (6) describes the evolution of the isotropic portion of the distribution function. The main objective in the present paper is the nature of the steady-state distributions as determined by the choice of $D_2(v)$ as well as the relaxation properties of the system towards a steady-state distribution as a function of α and the mass ratio M/m.

The steady distribution obtained by setting $\partial f/\partial t = 0$ in Eq. (6) is given by

$$\frac{df_{ss}(x)}{f_{ss}(x)} = -\left[\frac{2x}{1+\alpha v_{th}x^3\frac{D_2(v_{th}x)}{\hat{D}_1(z)}}\right]dx, \quad (7)$$

where

$$\hat{D}_1(z) = \mathrm{erf}(z) - \frac{2z}{\sqrt{\pi}}e^{-z^2}, \quad (8)$$

$v_{th} = \sqrt{2kT_b/m}$, $z = \sqrt{\gamma}x$, and $\gamma = M/m$. It is clear from Eq. (7) that the steady distribution is a Maxwellian for $\alpha = 0$, that is in the absence of wave-particle interactions. For $\alpha \neq 0$, the steady distribution is a non-Maxwellian distribution, the features of which also depend on the mass ratio γ. The Coulomb cross section that varies as $1/g^4$, where $\mathbf{g}$ is the relative velocity of two charged particles in a collision, does not appear explicitly. As a consequence of the additional diffusion term, the steady-state solution of Eq. (6), $f_{ss}(v)$, is no longer a Maxwellian distribution and depends on the ratio of the strength of the wave-particle diffusion term relative to the strength of Coulomb collisional relaxation; that is, on β, as well as the mass ratio m/M. The velocity dependence of this steady-state distribution function depends on both $\hat{D}_1(z)$ and $D_2(v_{th}x)$. It is this mass-dependent dimensionless diffusion coefficient that controls the Coulomb relaxation to equilibrium and the features of $f_{ss}(x)$.

It is useful to examine the dependence of $\hat{D}_1(\sqrt{\gamma}x)$ versus x. It is easy to see that, for $x \to \infty$, $\hat{D}_1(\sqrt{\gamma}x) \to 1$, and for small x,

$$\lim_{z\to 0}\hat{D}_1(z) \approx \frac{4}{3\sqrt{\pi}}\gamma^{3/2}x^3.$$

A dimensionless collision frequency $\nu(x) = \frac{3}{4z^3\sqrt{pi}}D_1(z)/(4z^3)$ can be defined. It is this strong mass dependence that controls both the approach to a steady state and the features of the steady-state distribution that are emphasized in the present paper. It is easy to see that, in the limit $\gamma \to \infty$, $\hat{D}_1(z) \to 1$ and with $D_2(v_{th}x) = 1/(v_{th}x)$, the steady distribution function is then defined by

$$\frac{df_\kappa(x)}{f_\kappa(x)} = -\frac{2x}{1+\alpha x^2}dx, \quad (9)$$

which can be recognized as the ordinary differential equation that defines the Kappa distribution (2), with $\kappa = (1-\alpha)/\alpha$. This result arises owing to the particular speed dependence of the drift and diffusion coefficients in the Fokker-Planck equation that gives Eq. (9). This result does not arise owing to long-range forces [33], nonextensive thermostatics [31,33], indeterminacy [25], a collisionless weakly coupled plasma far from equilibrium [27,28]), multiplicative noise [34], nonextensive entropy [20,21,26,28–30] or Levy flights [35].

The analysis by Yoon *et al.* [42] and Kim *et al.* [41], although based on the detailed physics of the interaction of electrons with Whistler-type waves, reduces to the ratio of the drift coefficient relative to the diffusion coefficient that varies as Eq. (7) that leads to a Kappa distribution. The section that follows presents some numerical results that further demonstrate the range of nonequilibrium distributions with this simple model for which only a subset are Kappa distributions. The works by Ma and Summers [38] for Whistler waves and Hasegawa *et al.* [39] for a radiation field use similar Fokker-Planck equations with drift and diffusion coefficients that yield the same ordinary differential equation for the steady-state distribution as in Eq. (9). Similarly, the analysis of anomalous diffusion in an optical lattice by Lutz gives a Kappa distribution with the appropriate ratio of the drift to diffusion coefficients as in Eq. (3) of Ref. [66] leading exactly to Eqs. (9) and (2) here.

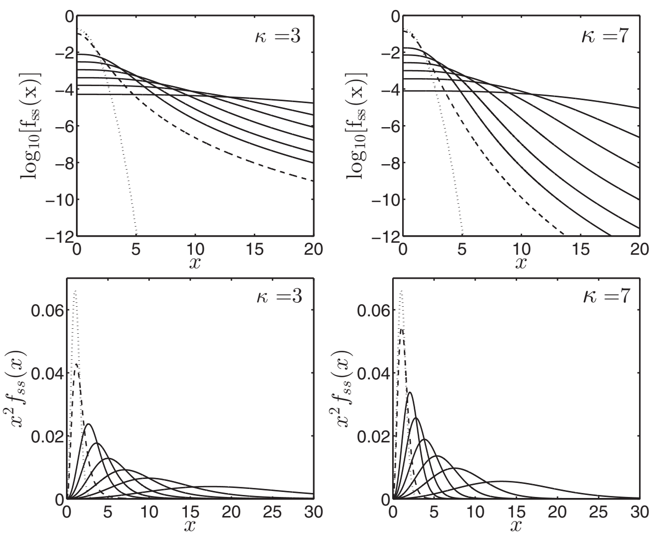

FIG. 1. The solid curves are the nonequilibrium steady-state distributions versus mass ratio $m/M = 500$, 160, 80, 40 20, and 10 from the topmost curve to the bottom curve approaching the Kappa distribution shown as the dashed curve for the wave-particle interaction Fokker-Planck equation. The Maxwellian is shown as the dotted curve.

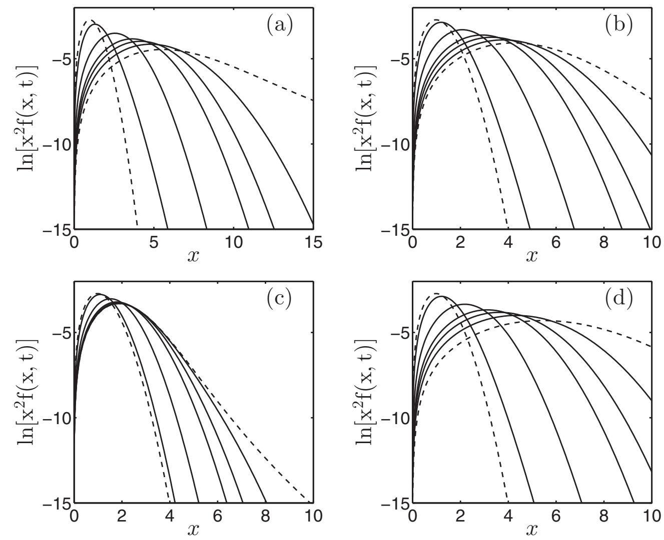

FIG. 2. Time dependence of the nonequilibrium distribution from an initial Maxwellian (innermost dashed curve) to the steady nonequilibrium distribution (outermost dashed curve) for the wave-particle interaction Fokker-Planck equation. (a) $\alpha = 1/4, \kappa = 3, \gamma = 50$, and successive reduced times are $t = 0.4$, 2, 6, 10, and 20. (b) $\alpha = 1/8$, $\kappa = 7, \gamma = 50$, (c) $\alpha = 1/8, \kappa = 7, \gamma = 8$, and (d) $\alpha = 1/10, \kappa = 9$, $\gamma = 100$, and the successive times are as in panel (a).

B. Numerical results

The steady-state nonequilibrium distribution from the Fokker-Planck equation (6) is given by Eqs. (7) and (8) and depends on the strength of the wave-particle diffusion operator denoted by α and the mass ratio $\gamma = M/m$ that defines the Coulomb diffusion coefficient. Only in the limit $\gamma \to \infty$ is this steady distribution function given by the Kappa distribution (9).

The variation of the steady nonequilibrium distribution given by Eq. (7) versus the mass ratio is shown in Fig. 1 as both $\log_{10}[x^2 f_{ss}(x)]$ and $x^2 f_{ss}(x)$ versus x for $\kappa = 3$ and 7, and mass ratios $m/M = 500$, 160, 80, 40, 20, and 10 from the topmost curve to the bottom curve approaching the Kappa distribution shown as the dashed curve. In Fig. 1, the distributions are plotted in the two forms one above the other with the same data. The upper graphs enhance the high energy portion of the distributions whereas the lower graphs demonstrate the position of the maxima of the distribution functions. The dotted curve is the Maxwellian whereas the dashed curve is the Kappa distribution for $\gamma \to \infty$. The solid curves are the steady distributions for finite mass ratio and represent distribution functions more energetic than the Kappa distribution. It is clear that the steady distribution is a strong function of the mass ratio and the distribution functions shown by the solid curves are not Kappa functions. Almost all of the published works giving Kappa distributions [38,39,42,44] are for the $m/M \to 0$ limit. The nonequilibrium distribution functions for finite m/M shown have extended "tails" in the high-x region, more so than for the Kappa distribution shown as the dashed line. The contrast between the Kappa distribution and the other mass-dependent distributions appears greater with variation of $x^2 f(x,t)$ versus x shown in the lower graphs in Fig. 1. The time-dependent distributions from the Fokker-Planck equation (6) are shown in Fig. 2 for several system parameters. The Chang-Cooper finite-difference algorithm was used to solve the Fokker-Planck equation (6) as discussed elsewhere [67,68]. The dashed curves show the initial Maxwellian and the energetic final nonequilibrium steady-state distributions. The features of the distribution functions should be viewed in conjunction with the change in the temperature and the Kullback-Leibler entropy shown in Fig. 3. In this figure, the system parameters are chosen to show the different heatings of the test particle owing to the wave particle interaction. Also shown is the time dependence of the Kullback-Leibler entropy for which $d\,\Sigma_{\rm KL}(t)/dt > 0$ and $\Sigma_{\rm KL}(t) \to 0$ as $t \to \infty$. Pezzi [9] has presented a similar time history for a nonlinear Landau collision operator based on the Boltzmann H theorem for a one component plasma (see Figs. 2 and 5 in this reference). We can conclude from these results that the Tsallis entropy plays no role in the determination of these time-dependent

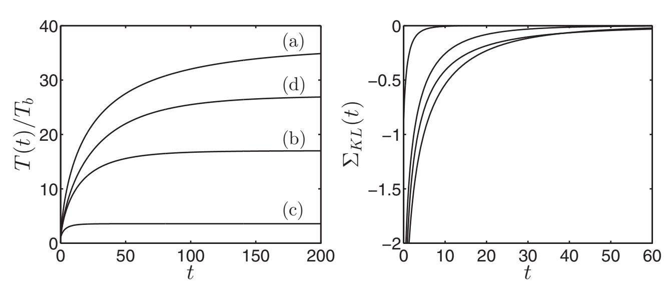

FIG. 3. Variation of the temperature ratio, $T(t)/T_b$, and the Kullback-Leibler entropy, $\Sigma_{\rm KL}(t)$, corresponding to the distributions in Fig. 2 for the wave-particle interaction Fokker-Planck equation. For the entropy, the curves are in the order (c), (b), (a), and (d) from top to bottom.

nonequilibrium distributions nor for the steady distributions that are not Kappa distributions.

III. ELECTRON TRANSPORT IN AN EXTERNAL ELECTRIC FIELD AND THE APPROACH TO A NONEQUILIBRIUM STEADY STATE

We consider the relaxation of electrons dilutely dispersed in a heat bath of atoms of mass M at constant temperature T_b and subject to an external uniform constant electric field E. Owing to the very small electron to moderator mass ratio m/M, the anisotropic part of the distribution function can be represented by a single Legendre polynomial; that is,

$$f(\mathbf{v},t) = f_0(v,t) + f_1(v,t)P_1(\theta), \tag{10}$$

where θ is the angle between $\mathbf{v}$ and the polar axis taken in the direction of the electric field. Equation (10) is the well-known two-term approximation [48,49,69].

The spherical portion of the electron distribution function $f_0(v,t)$ for this small-mass-ratio limit satisfies a linear Fokker-Planck equation with velocity-dependent drift and diffusion coefficients as defined by the electron-moderator momentum transfer cross section and the magnitude of the electric field. Similar Fokker-Planck equations have been used to study many different electron transport systems [70–72] including electron attachment [73,74].

A. Fokker-Planck equation

The coupled equations for the first two terms $f_0(v,t)$ and $f_1(v,t)$ are solved by replacing $f_1(v,t)$ in terms of $f_0(v,t)$ as described elsewhere [49,68,69]. The result is the Fokker-Planck equation for $f_0(v,t)$, given by

$$\frac{\partial f_0}{\partial t} = \frac{1}{x^2}\frac{\partial}{\partial x}\left[2x^4\sigma(x)f_0 + x^2B(x)\frac{\partial f_0}{\partial x}\right], \tag{11}$$

where

$$B(x) = x\sigma(x) + \frac{\beta^2}{x\sigma(x)}, \tag{12}$$

and the field strength parameter is $\beta^2 = (M/6m_e)(eE/nkT_b)^2$. Henceforth the spherical portion of the distribution $f(\mathbf{v},t)$, Eq. (10); namely, $f_0(v,t)$, is written as $f(x,t)$ with $v = v_{th}x$. The steady nonequilibrium electron distribution arising from an interplay of the acceleration in a steady electric field and moderated by electron-atom collisions is given by

$$f_{ss}(x) = C\exp\left[-2\int_0^x \frac{y^2\sigma}{B(y)}dy\right], \tag{13}$$

where C is a normalization. The dimensionless time $t = t'/\tau$ is defined by

$$\tau = \left[\frac{nm_e\sigma_0}{2M}\sqrt{\frac{2k_BT_b}{m_e}}\right]^{-1}, \tag{14}$$

where n_e is the density of the bath species and σ_0 is a convenient hard sphere cross section. The distribution function $f_{ss}(x)$ given by Eq. (13) is often referred to as the Davydov distribution [68,75,76] and denoted by $D(x)$.

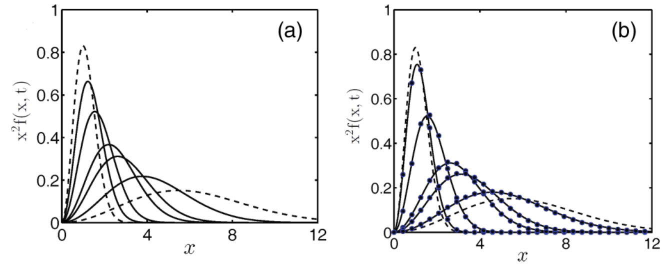

FIG. 4. Time-dependent distribution function, $f(x,t)$ versus x for different t, for the e-atom Fokker Planck equation. The dashed curves are the initial Maxwellian distribution with $T(0)/T_b = 30$ and the final Maxwellian distribution with $T(0)/T_b = 1$. (a) $p = 0$; $t/\tau = 2$, 4 5, 7.5, and 10 (b) $p = 1$; $t/\tau = 0.5$, 1.0, 1.5, 2.5, and 3.75 and the symbols show the Maxwellian distribution parametrized by $T(t)$. The results are for the field-free case and $\beta = 0$.

In this paper, model systems are used so as to better understand the manner in which the speed dependence of the cross section affects the details of the time-dependent nonequilibrium distributions and the steady-state distributions. A reduced model cross section of the form $\sigma(x) = \sigma_0/x^p$ is chosen and the relaxation behavior versus p is studied. The systems with $p = 0$ and 1 correspond to the hard sphere and Maxwell molecule cross sections, respectively. The cross section with $p = 2$ and finite β leads to the ordinary differential equation given by

$$\frac{df_{ss}(x)}{f_{ss}(x)} = -\frac{2x}{1+\beta^2x^2}dx, \tag{15}$$

analogous to Eq. (9) which are the defining equations for the Kappa distribution (2) with $\kappa = (1-\beta^2)/\beta^2$. For $\kappa > 3/2$, $\beta \leqslant \sqrt{2/5}$. Although not central to the current objectives, we briefly include the steady-state solution with $p = 3$ which can be shown to be given by

$$f_{ss}(x) = C(\beta)\exp\left[-\frac{1}{\beta}\tan^{-1}\left(\beta x^2\right)\right], \tag{16}$$

which exhibits infinitely long hot "tails" that do not decay to zero. There is some experimental and theoretical evidence of power law cross sections [77,78]. This and other aspects of the Fokker-Planck equations introduced here will be studied further in a forthcoming presentation.

B. Numerical results

Figures 4(a) and 4(b) show the time evolution of an initial Maxwellian distribution at temperature $T(0) = 30T_b$ for $p = 0$ and $p = 1$, respectively. The time-dependent distributions are determined with the Chang-Copper [1,68] finite-difference solution of Eq. (11) [68,76]. It is this mass-dependent dimensionless diffusion coefficient that controls the Coulomb relaxation to equilibrium and the features of $f_{ss}(x)$. The case with $p = 0$ corresponds to a hard sphere momentum transfer cross section whereas, for $p = 1$, the cross section corresponds to the Maxwell molecule cross section. The initial and final Maxwellian distributions are shown as the dashed curves. The other distributions are at different times as given in the caption. Figure 4(b) with $p = 1$ is for the Maxwell molecule cross section and belongs to the class of systems

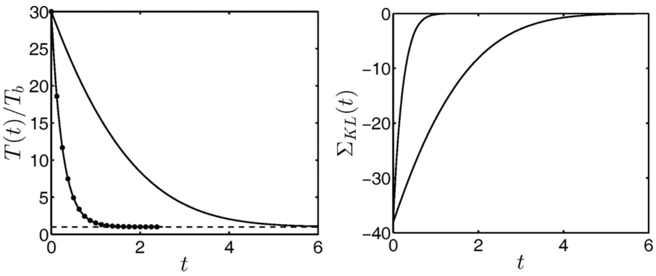

FIG. 5. The variation of the temperature, $T(t)/T_b$, and the Kullback-Leibler entropy, $\Sigma_{\rm KL}(t)$, for $p = 0$ and $p = 1$ corresponding to the distribution functions in Fig. 4. The relaxation is slower for $p = 1$.

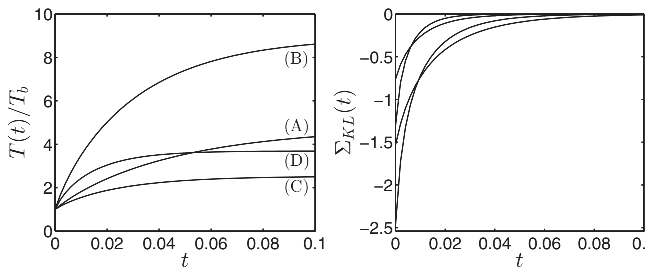

FIG. 7. Time variation of $T(t)/T_b$ and $\Sigma_{\rm KL}(t)$ for the distributions in Fig. 6. The temperature curves are labeled as in the previous figure. For the Kullback-Leibler entropy, the upper portions of the curves near steady state are ordered from top to bottom with $(p,\beta) = (1,12)$, (1,6), (0,12), and (0,6).

which exhibit canonical invariance [79]. As a consequence, the intermediate distributions are also Maxwellian at the time-dependent temperature $T(t)$, which varies with time t as a pure exponential. The solid curves represent the solutions of the Fokker-Planck equation as described whereas the symbols show a Maxwellian distribution evaluated with $T(t)$.

The time variation of $T(t)/T_b$ for the system variables shown in the caption of Fig. 5 is on the left-hand side (LHS) of the figure. The curve for $T(t)/T_b$ with the symbols is the pure exponential decay which coincides exactly with the temperature of the time-dependent distribution obtained with the Fokker-Planck equation which is shown as the solid curve. This behavior is a consequence of the particular property of this Fokker-Planck equation that exhibits canonical invariance [79]; namely, the preservation of a Maxwellian distribution with a time-dependent temperature. The variation of the Kullback-Leibler entropy for these distributions is also shown in Fig. 5 with $d\Sigma_{\rm KL}(t)/dt > 0$ and $\Sigma_{\rm KL}(t) \to 0$ as $t \to \infty$.

The time-dependent distribution functions for $p = 0$ and $p = 1$ are shown in Fig. 6 for two different dimensionless electric field strengths, $\beta = 6$ and 12, respectively. The heating of the distribution is evident in all cases and is largest for $(p,\beta) = (0,12)$ and smallest for $(p,\beta) = (1,6)$ as shown by the temperature increase in Fig. 7. The monotonic growth of the Kullback-Leibler entropy, $\Sigma_{\rm KL}(t)$, is also shown in Fig. 7 consistent with $d\Sigma_{\rm KL}(t) > 0$ and $\Sigma_{\rm KL}(t) \to 0$ as $t \to \infty$. The steady-state nonequilibrium distributions, also shown in Fig. 6 with dashed curves, are not Kappa distributions. For the hard sphere cross section, the distribution function for large electric

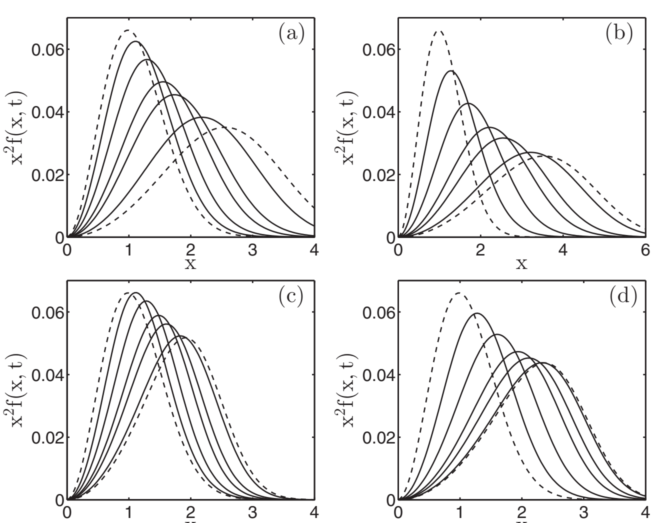

FIG. 6. Time-dependent distribution function, $x^2 f(x,t)$, versus x for different t. The dashed curves are the initial Maxwellian distribution with $T(0)/T_b = 1$ and the final nonequilibrium steady-state distribution. The e-atom cross section is $\sigma(x) = \sigma_0/x^p$ and the dimensionless electric field strength is β. (a) $p = 0$, $\beta = 6$, (b) $p = 0$, $\beta = 12$, (c) $p = 1$, $\beta = 6$, and (d) $p = 1$, $\beta = 12$; the five solid curves are the distribution functions for the reduced times, t/τ equal to 0.004, 0.008, 0.032, 0.048, and 0.12.

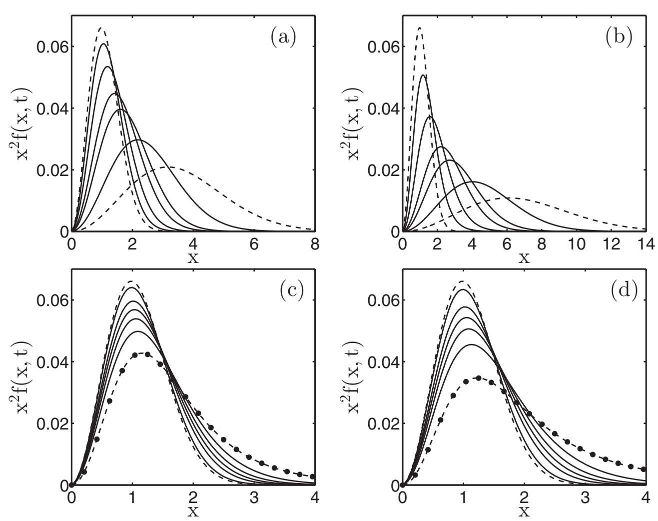

FIG. 8. Time-dependent distribution function, $x^2 f(x,t)$ versus x for different t. The dashed curves are the initial Maxwellian distribution with $T(0)/T_b = 1$ and the final nonequilibrium steady-state distribution. The e-atom cross section is $\sigma(x) = \sigma_0/x^p$ and the dimensionless electric field strength is α_2. (a) $p = 1$, $\beta = 6$. (b) $p = 1$, $\beta = 12$ the five solid curves for panels (a) and (b) are the distribution functions for the reduced times $t/t_0 = 0.01$, 0.02, 0.04, 0.06, and 0.15, respectively. (c) $p = -2$, $\beta = 0.5$, $\kappa = 3$ and (d) $p = 2$, $\beta = 1/\sqrt{3}$, $\kappa = 2$; the five solid curves for panels (c) and (d) are the distribution functions for the reduced times $t/t_0 = 0.04$, 0.15, 0.25, 0.4, and 0.75, respectively. The solid symbols in panels (c) and (d) represent the Kappa distribution calculated with Eq. (2).

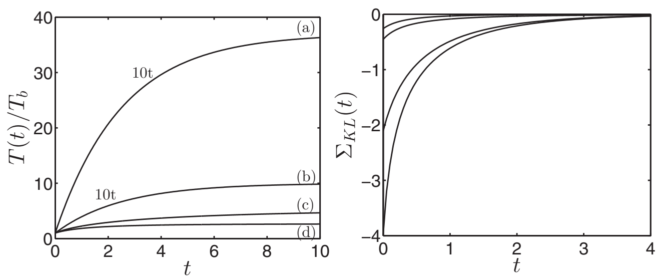

FIG. 9. Time variation of $T(t)/T_b$ for the distributions in Fig. 8 and labeled as in the previous figure. For the curves labeled (a) and (b), the time axis should be divided by 10. The curves correspond to system variables according to (a) $p = 1, \beta = 3$, (b) $p = 1, \beta = 6$, (c) $p = 2, \beta = 0.5, \kappa = 3$, and (d) $p = 2, \beta = 1/\sqrt{3}, \kappa = 2$. For $\Sigma_{\rm KL}(t)$, the curves from top to bottom correspond to (d), (c), (b), and (a) and the timescale factor is as for the temperature relaxation.

field strengths ($\beta \to \infty$) tends to a Druyvesteyn distribution which varies as $x^2 e^{-cx^4}$ [75,76], where c is a constant.

A comparison of the time dependence of the distribution functions for $p = 1$ and $p = 2$ is shown in Figs. 8(a) and 8(b) with $p = 1$ and $p = 2$ for Figs. 8(c) and 8(d). The time-dependent approach to this steady Davydov distribution which coincides with the Kappa distribution is also provided in terms of the Kullback-Leibler relative entropy, as shown in Fig. 9 and discussed later. The important feature to point out is that the steady distributions for $p = 2$ in Figs. 9(c) and 9(d) are Kappa distributions given by Eq. (15). The symbols on the dashed curves are the values of the Kappa distribution calculated with Eq. (2). This is consistent with the result in Sec. III A that gave the Kappa distribution. It is interesting that the heating by the electric field is greater for $p = 1$ than for $p = 2$ because the relaxation rate is slower. This is corroborated in Fig. 9 which shows that the t variation of $T(t)/T_b$ with the largest heating for $p = 1$. The relaxation rate is also faster for $p = 1$ than for $p = 2$. The approach to a steady-state distribution, be it a Kappa distribution as in Figs. 8(c) and 8(d) or as a general Davydov distribution as in Figs. 8(a) and 8(b) is rationalized with the Kullback-Leibler entropy shown in Fig. 9.

A comparison of the time dependence of the distribution functions for $p = 1$ and $p = 2$ is shown in Fig. 8 with $p = 1$ for Figs. 8(a) and 8(b) and $p = 2$ for Figs. 8(c) and 8(d). The time-dependent approach to this steady Davydov distribution which coincides with the Kappa distribution is also provided in terms of the Kullback-Leibler relative entropy, as shown in Fig. 9 and discussed later. The important feature to point out is that the steady distributions for $p = 2$ in Figs. 9(c) and 9(d) are Kappa distributions as defined by Eq. (15). The symbols on the dashed curves are the values of the Kappa distribution calculated with Eq. (2). This is consistent with the result in Sec. III A that gave the Kappa distribution. It is interesting that the heating by the electric field is greater for $p = 1$ than for $p = 2$ because the relaxation rate is slower. This is corroborated in Fig. 9 which shows that the t variation of $T(t)/T_b$ with the largest heating for $p = 1$. The relaxation rate is also faster for $p = 1$ than for $p = 2$. The approach to a steady-state distribution, be it a Kappa distribution as in Figs. 8(c) and 8(d) or as a general Davydov distribution as in Figs. 8(a) and 8(b) is rationalized with the Kullback-Leibler entropy shown in Fig. 9.

IV. SUMMARY

This paper has considered the nonequilibrium effects in two different systems, each parametrized with two variables. Each system involves the time evolution of the translational distribution function for a minor test particle in contact with a heat bath at constant temperature. The first system considers a Fokker-Planck equation for the distribution function of a test particle subject to wave-particle interactions mediated by Coulomb collisions with heat bath particles. The time evolution and the steady-state distributions are dependent on the particle mass ratio and the strength of the wave-particle interaction α perturbing the system from equilibrium. The steady-state distributions can generally be considered as Davydov distributions [75,76] and are Kappa distributions in the limit for the test particle to heat bath particle mass ratio, $m/M \to 0$.

The second system considers a model system for electron transport in an external electric field of dimensionless strength β. The electron-atom momentum transfer cross section is taken to be a power law, $\sigma(x) = \sigma_o/x^p$. The time-dependent distributions of electrons for different field strengths and versus the parameter p are determined from the appropriate Fokker-Planck equation. The nonequilibrium steady-state distributions vary considerably with β and p and are generally Davydov distributions and become Kappa distributions only for $p = 2$. The approach to a steady-state distribution is rationalized in every case with the Kullback-Leibler entropy.

This steady-state Kappa distributions calculated in this paper do not require many of the physical attributes discussed by numerous authors on the subject of Kappa distributions and nonextensive entropy. The systems in this paper that yield Kappa distributions in a certain limited parameter space are not necessarily parametrized by long-range interactions [33], Levy random walks [35], multiplicative noise [34], collisionless plasmas [27,28], nonextensive thermostatics [31,32], indeterminacy [25], etc. In particular, the Tsallis entropy functional has only one parameter and cannot describe the multitude of nonequilibrium distributions in the parameter space of these two system.

ACKNOWLEDGMENT

This research was supported with a grant (No. 03913) from the Natural Sciences and Engineering Research Council of Canada (NSERC).

[1] S. Chapman and T. G. Cowling, *The Mathematical Theory of Nonuniform Gases* (Cambridge University Press, Cambridge, 1970).

[2] S. R. de Groot and P. Mazur, *Non-Equilibrium Thermodynamics* (Dover, New York, 1984).

[3] P. M. Bellan, *Fundamentals of Plasma Physics* (Cambridge University Press, Cambridge, 2006).
[4] J. Ross and P. Mazur, Some deductions from a formal statistical mechanical theory of chemical kinetics, J. Chem. Phys. **35**, 91 (1961).
[5] B. Shizgal and M. Karplus, Nonequilibrium contributions to the rate of reaction. I. Perturbation of the velocity distribution function, J. Chem. Phys. **52**, 4262 (1970).
[6] B. Shizgal and J. C. Barrett, Time dependent nucleation, J. Chem. Phys. **91**, 6506 (1989).
[7] M. A. Durán-Olivencia and J. F. Lutsko, Unification of classical nucleation theories via a unified Itô-Stratonovich stochastic equation, Phys. Rev. E **92**, 032407 (2015).
[8] F. J. Fahr and B. Shizgal, Modern exospheric theories and their observational relevance, Rev. Geophys. **21**, 75 (1983).
[9] O. Pezzi, Solar wind collisional heating, J. Plasma Phys. **83**, 555830301 (2017).
[10] M. Torrilhon and H. Struchtrup, Regularized 13-moment equations: Shock structure calculations and comparison to Burnett model, J. Fluid Mech. **513**, 171 (2004).
[11] M. M. R. Williams, *The Slowing Down and Thermalization of Neutrons* (North-Holland, Amsterdam, 1966).
[12] E. A. Mason and E. W. McDaniel, *Transport Properties of Ions in Gases* (Wiley, New York, 1988).
[13] L. A. Viehland, Uniform moment theory for charged particle motion in gases. 2. Second approximation, J. Stat. Phys. **163**, 175 (2016).
[14] C. S. Kim and B. Shizgal, Relaxation of hot-electron distributions in GaAs, Phys. Rev. B **44**, 2969 (1991).
[15] C. Jacoboni, *Theory of Electron Transport in Semiconductors* (Springer, Berlin, 2010).
[16] S. Chandrasekhar, Brownian motion, dynamical friction, and stellar dynamics, Rev. Mod. Phys. **21**, 383 (1949).
[17] J. Binney and S. Tremaine, *Galactic Dynamics*, 2nd ed. (Princeton University Press, New Jersey, 2008).
[18] D. Sornette, *Critical Phenomena in Natural Sciences* (Springer, London, 2006).
[19] M. E. J. Newman, Power laws, Pareto distributions and Zipf's law, Contemp. Phys. **46**, 323 (2005).
[20] C. Tsallis, Possible generalization of Boltzmann–Gibbs statistics, J. Stat. Phys. **52**, 479 (1988).
[21] C. Tsallis, Non–extensive thermostatics: Brief review and comments, Physica A (Amsterdam, Neth.) **221**, 277 (1995).
[22] C. Tsallis, The nonadditive entropy S_q and its application in physics and elsewhere: Some remarks, Entropy **13**, 1765 (2011).
[23] H. Grad, On Boltzmann's H-theorem, J. Soc. Indust. Appl. Math **13**, 259 (1965).
[24] N. Meyer-Vernet, Large scale structure of planetary environments: The importance of not being Maxwellian, Planet. Space Sci. **49**, 247 (2001).
[25] M. P. Leubner and Z. Vörös, A nonextensive entropy approach to solar wind intermittency, Astrophys. J. **618**, 547 (2005).
[26] G. Livadiotis and D. J. McComas, Beyond Kappa distributions: Exploiting Tsallis statistical mechanics in space plasmas, J. Geophys. Res. **114**, A11105 (2009).
[27] V. Pierrard and V. Lazar, Kappa distributions; Theory and applications in space plasmas, Solar Phys. **267**, 153 (2010).
[28] G. Livadiotis and D. J. McComas, Understanding Kappa distributions: A toolbox for space science and astrophysics, Space Sci. Rev. **175**, 183 (2013).
[29] G. Livadiotis, *Kappa Distributions* (Elsevier, Amsterdam, 2017).
[30] G. Livadiotis, Derivation of the entropic formula for the statistical mechanics of space plasmas, Nonlinear Proc. Geophys. **25**, 77 (2018).
[31] M. P. Leubner, A nonextensive entropy approach to Kappa-distributions, Astrophys. Space Sci. **282**, 573 (2002).
[32] M. P. Leubner, Fundamental issues on kappa-distributions in space plasmas and interplanetary proton distributions, Phys. Plasmas **11**, 1308 (2004).
[33] M. P. Leubner, Consequences of entropy bifurcation in non–Maxwellian astrophysical environments, Nonlinear Proc. Geophys. **15**, 531 (2008).
[34] T. S. Biró and A. Jakovác, Power-Law Tails from Multiplicative Noise, Phys. Rev. Lett. **94**, 132302 (2005).
[35] M. R. Collier, Are magnetospheric suprathermal particle distributions (κ functions) inconsistent with maximum entropy considerations, Adv. Space Res. **33**, 2108 (2004).
[36] M. Leitner, Z. Vörös, and M. P. Leubner, Introducing log-kappa distributions for solar wind analysis, J. Geophys. Res. **114**, A12104 (2009).
[37] S. Zaheer and P. H. Yoon, On quiet-time solar wind electron distributions in dynamical equilibrium with Langmuir turbulence, Astrophys. J. **775**, 108 (2013).
[38] C.-Y. Ma and D. Summers, Formation of power-law energy spectra in space plasmas by stochastic acceleration due to whistler-mode waves, Geophys. Res. Lett. **26**, 1121 (1999).
[39] A. Hasegawa, K. Mima, and M. Duong-van, Plasma Distribution Function in a Superthermal Radiation Field, Phys. Rev. Lett. **54**, 2608 (1985).
[40] M. Lazar, H. Fichtner, and P. H. Yoon, On the interpretation and applicability of κ-distributions, Astron. Astrophys. **589**, A39 (2016).
[41] S. Kim, P. H. Yoon, G. S. Choe, and L. Wang, Asymptotic theory of solar wind electrons, Astrophys. J. Lett. **806**, 32 (2015).
[42] P. H. Yoon, S. Kim, G. S. Choe, and Y.-J. Moon, Revised model of the steady–state solar wind halo electron velocity distribution function, Astrophys. J. Lett. **826**, 204 (2016).
[43] E. Lutz, Power-Law Tail Distributions and Nonergodicity, Phys. Rev. Lett. **93**, 190602 (2004).
[44] P. H. Yoon, Electron Kappa distribution and quasi-thermal noise, J. Geophys. Res. **119**, 7074 (2014).
[45] B. D. Shizgal, Coulomb collisional processes in space plasmas; relaxation of suprathermal particle distributions, Planet. Space Sci. **52**, 923 (2004).
[46] B. D. Shizgal, Suprathermal particle distributions in space physics: Kappa distributions and entropy, Astrophys. Space Sci. **312**, 227 (2007).
[47] M. Tumminello, F. Lillo, and R. N. Mantegna, Kullback-Leibler distance as a measure of the information filtered from multivariate data, Phys. Rev. E **76**, 031123 (2007).
[48] D. R. A. McMahon and B. Shizgal, Hot-electron zero-field mobility and diffusion in rare-gas moderators, Phys. Rev. A **31**, 1894 (1985).
[49] B. Shizgal and D. R. A. McMahon, Electric field dependence of transient electron transport properties in rare gas moderators, Phys. Rev. A **32**, 3669 (1985).
[50] J. P. Boon and C. Tsallis, Special issue overview Nonextensive statistical mechanics: new trends, new perspectives, Europhys. News **36**, 185 (2005).

[51] B. R. La Cour and W. C. Schieve, Tsallis maximum entropy principle and the law of large numbers, Phys. Rev. E **62**, 7494 (2000).

[52] A. Cho, A fresh take on disorder, or disorderly science? Science **297**, 1268 (2002).

[53] M. Nauenberg, Critique of q-entropy for thermal statistics, Phys. Rev. E **67**, 036114 (2003).

[54] C. Tsallis, Comment on critique of q-entropy for thermal statistics, Phys. Rev. E **69**, 038101 (2004).

[55] M. Nauenberg, Reply to "comment on critique of q-entropy for thermal statistics,"Phys. Rev. E **69**, 038102 (2004).

[56] D. H. Zanette and M. A. Montemurro, A note on the non-thermodynamical applications of non-extensive entropy, Phys. Lett. A **324**, 383 (2004).

[57] R. Balian and M. Nauenberg, Comment on the paper by A. Rapisarda and A. Pluchino, Europhys. News. **36**, 202 (2005), Letter to the editors, Europhys. News. **37**, 9 (2006).

[58] F. Bouchet, T. Dauxois, and S. Ruffo, Comment on the paper by A. Rapisarda and A. Pluchino, Europhys. News **36**, 202 (2005), Letter to the editors, Europhys. News. **37**, 9 (2006).

[59] J. F. Lutsko and J. P. Boon, Questioning the validity of non-extensive thermodynamics for classical Hamiltonian systems, Europhys. Lett. **95**, 20006 (2011).

[60] J. Cartwright, Roll over, Boltzmann, Phys. World **27**, 31 (2014).

[61] L. J. Spitzer, *Physics of Fully Ionized Gases* (Interscience, New York, 1962).

[62] F. L. Hinton, Collisional Transport in Plasma, in *Handbook of Physics, Basic Plasma Physics*, edited by A. A. Galeev, R. Z. Sagdeev (Elsevier, The Netherlands, 1983), pp. 147–197.

[63] T. H. Stix, *Waves in Plasmas* (Springer, New York, 1992).

[64] D. R. Nicholson, *Introduction to Plasma Theory* (Wiley, New York, 1983).

[65] R. M. Kulsrud, *Plasma Physics for Astrophysics* (Princeton University Press, Princeton, 2005).

[66] E. Lutz, Anomalous diffusion and Tsallis statistics in an optical lattice, Phys. Rev. A **67**, 051402 (2003).

[67] J. C. Chang and G. Cooper, A practical difference scheme for Fokker-Planck equations, J. Comput. Phys. **6**, 1 (1970).

[68] K. Leung, B. D. Shizgal, and H. Chen, The quadrature discretization method QDM in comparison with other numerical methods of solution of the Fokker-Planck equation for electron thermalization, J. Math. Chem. **24**, 291 (1998).

[69] L. C. Pitchford and A. V. Phelps, Comparative calculations of electron-swarm properties in N_2 at moderate E/N values, Phys. Rev. A **25**, 540 (1982).

[70] L. Demeio and B. Shizgal, A uniform Wentzel-Kramers-Brillouin approach to electron transport in molecular gases, J. Chem. Phys. **99**, 7638 (1993).

[71] B. Shizgal, D. R. A. McMahon, and L. A. Viehland, Thermalization of electrons in gases, Int. J. Radiat. Appl. Instrum. Part C. Radiat. Phys. Chem. **34**, 35 (1989).

[72] B. D. Shizgal and K. Kowari, Electron attachment kinetics coupled to electron thermalization in SF_6/Ar mixtures, J. Phys. D: Appl. Phys. **35**, 973 (2002).

[73] K. Kowari, L. Demeio, and B. Shizgal, Electron degradation and thermalization in CH_4 gas, J. Chem. Phys. **97**, 2061 (1992).

[74] K.-I. Kowari, K. Leung, and B. D. Shizgal, The coupling of electron thermalization and electron attachment in CCl_4/Ar and CCl_4/Ne mixtures, J. Chem. Phys. **108**, 1587 (1998).

[75] M. J. Bell and M. D. Kostin, Transport coefficients and energy distributions of electrons in gases, Phys. Rev. **169**, 150 (1968).

[76] G. H. Wannier, Derivation of the Davydov distribution from the Boltzmann equation, Am. J. Phys. **39**, 281 (1971).

[77] J. M. Urbassek and U. Conrad, Collision cascades in binary media: Analytical results for power-law cross sections, Nucl. Instrum. Methods Phys. Res., Sect. B **B69**, 413 (1992).

[78] V. Kuzmin and P. Sigmund, Exploring reciprocity as a tool in low-energy selectronic stopping, Nucl. Instrum. Methods Phys. Res., Sect. B **B269**, 817 (2011).

[79] H. C. Andersen, I. Oppenheim, K. E. Shuler, and G. H. Weiss, Exact condition for the preservation of a canonical distribution in Markovian relaxation process, J. Math. Phys. **5**, 522 (1964).